

Cramér-Rao bounds and TX-RX selection in a multistatic radar scenario

M. Greco, P. Stinco, F. Gini
Dept. of “Ingegneria dell’Informazione”
University of Pisa
Pisa, Italy

A. Farina
SELEX Sistemi Integrati
Rome, Italy

M. Rangaswamy
Air Force Research Laboratory Sensors Directorate,
80 Scott Dr. Hanscom Air Force Base, MA 01731-2909, USA

Abstract—Multistatic radars utilize multiple transmitter and receiver sites to provide several different monostatic and bistatic channels of observation. Multistatic passive and active systems can offer many advantages in terms of coverage and accuracy in the estimation of target signal parameters but unfortunately their performances are heavily sensitive to the position of receivers (RX) and transmitters (TX) with respect to the target trajectory. As known, geometry factors play an important role in the shape of the ambiguity function (AF) which is often used to measure the possible global resolution and large error properties of the target parameters estimates. Exploiting the relation between the ambiguity function and the Cramér-Rao lower bound (CRLB), in this work we propose an algorithm for choosing in a multistatic scenario, along the trajectory of the tracked target, the pair TX-RX with the best asymptotic performance calculated in terms of CRLB on estimation accuracy.

I. INTRODUCTION

Recently, great interest has been devoted to systems making use of illuminators of opportunity, such as broadcast or communications signals, tracking targets by range and Doppler information. These techniques are known as Passive Coherent Location (PCL), and have the advantage that the receivers do not need any transmitter hardware of their own, and are completely passive, and hence undetectable. Among all the transmitters of opportunity available in the environment, broadcast transmitters represent some of the most attractive for surveillance purposes, owing to their high powers and excellent coverage.

Furthermore, Passive Coherent Location techniques can be extended to Multistatic radar systems where multiple transmitter and receiver sites are used to provide several different bistatic channels of observation, leading to an increase in the information on a particular area of surveillance. The information gain obtained through this spatial diversity can give rise to a number of advantages in typical radar functions, such as detection, parameter estimation, tracking and identification. The performance of each bistatic channel heavily depends upon the geometry of the scenario and the

position of the target with respect to each receiver and transmitter.

In this paper we approach the problem of optimally selecting the transmitter-receiver (TX-RX) pair, through calculation of the ambiguity function (AF) and of the Cramér-Rao lower bounds (CRLBs) for the bistatic geometry of each TX-RX pair. The best pair is defined as that exhibiting the lowest bistatic CRLB for the target velocity or range. These results can be used for the dynamical selection of the TX-RX signals for the tracking of a radar target moving along a trajectory in a multistatic scenario. The multistatic scenario analyzed in this work is composed by a transmitter and four receivers. The results reported here have been obtained considering a single frequency modulated (FM) commercial radio station as transmitter of opportunity [1].

II. BISTATIC GEOMETRY

Before starting our study, it is necessary to describe the coordinate system used to represent a bistatic radar geometry. Figure 1 shows the coordinate system and its parameters. The positions of the TX, RX and target are generic. Considering an ordinary Cartesian grid, the TX is located at point T_x , whose coordinates are (x_T, y_T) , the RX is at point R_x in (x_R, y_R) and the target is located at point B , whose coordinates are (x, y) .

The triangle formed by the transmitter, the receiver and the target is called the bistatic triangle. As shown in Figure 1, the sides of the bistatic triangle are R_T , R_R and L , where R_T is the range from transmitter to target, R_R is the range from receiver to target and L is the baseline between the transmitter and the receiver. The internal angles of the bistatic triangle that, without lack of generality, are assumed to be positive, are α , δ and γ . In particular, the bistatic angle δ is the angle at the apex of the bistatic triangle, at the vertex which represents the target. Assuming that the coordinates of the transmitter, the receiver and the target are known, it is possible to calculate all the parameters of the bistatic triangle. θ_T and θ_R are the look angle of the transmitter and the look angle of the receiver, respectively, they are measured positive clockwise from the vector normal to the baseline pointing forward the target.

This work has been partially funded by EOARD grant FA8655-07-1-3096

Report Documentation Page

Form Approved
OMB No. 0704-0188

Public reporting burden for the collection of information is estimated to average 1 hour per response, including the time for reviewing instructions, searching existing data sources, gathering and maintaining the data needed, and completing and reviewing the collection of information. Send comments regarding this burden estimate or any other aspect of this collection of information, including suggestions for reducing this burden, to Washington Headquarters Services, Directorate for Information Operations and Reports, 1215 Jefferson Davis Highway, Suite 1204, Arlington VA 22202-4302. Respondents should be aware that notwithstanding any other provision of law, no person shall be subject to a penalty for failing to comply with a collection of information if it does not display a currently valid OMB control number.

1. REPORT DATE MAY 2010	2. REPORT TYPE	3. DATES COVERED 00-00-2010 to 00-00-2010			
4. TITLE AND SUBTITLE Cramer-Rao bounds and TX-RX selection in a multistatic radar scenario		5a. CONTRACT NUMBER			
		5b. GRANT NUMBER			
		5c. PROGRAM ELEMENT NUMBER			
6. AUTHOR(S)		5d. PROJECT NUMBER			
		5e. TASK NUMBER			
		5f. WORK UNIT NUMBER			
7. PERFORMING ORGANIZATION NAME(S) AND ADDRESS(ES) Air Force Research Laboratory, Sensors Directorate, 80 Scott Dr, Hanscom AFB, MA, 01731-2909		8. PERFORMING ORGANIZATION REPORT NUMBER			
9. SPONSORING/MONITORING AGENCY NAME(S) AND ADDRESS(ES)		10. SPONSOR/MONITOR'S ACRONYM(S)			
		11. SPONSOR/MONITOR'S REPORT NUMBER(S)			
12. DISTRIBUTION/AVAILABILITY STATEMENT Approved for public release; distribution unlimited					
13. SUPPLEMENTARY NOTES See also ADM002322. Presented at the 2010 IEEE International Radar Conference (9th) Held in Arlington, Virginia on 10-14 May 2010. Sponsored in part by the Navy.					
14. ABSTRACT Multistatic radars utilize multiple transmitter and receiver sites to provide several different monostatic and bistatic channels of observation. Multistatic passive and active systems can offer many advantages in terms of coverage and accuracy in the estimation of target signal parameters but unfortunately their performances are heavily sensitive to the position of receivers (RX) and transmitters (TX) with respect to the target trajectory. As known, geometry factors play an important role in the shape of the ambiguity function (AF) which is often used to measure the possible global resolution and large error properties of the target parameters estimates. Exploiting the relation between the ambiguity function and the Cram?Rao lower bound (CRLB), in this work we propose an algorithm for choosing in a multistatic scenario, along the trajectory of the tracked target, the pair TX-RX with the best asymptotic performance calculated in terms of CRLB on estimation accuracy.					
15. SUBJECT TERMS					
16. SECURITY CLASSIFICATION OF:			17. LIMITATION OF ABSTRACT Same as Report (SAR)	18. NUMBER OF PAGES 6	19a. NAME OF RESPONSIBLE PERSON
a. REPORT unclassified	b. ABSTRACT unclassified	c. THIS PAGE unclassified			

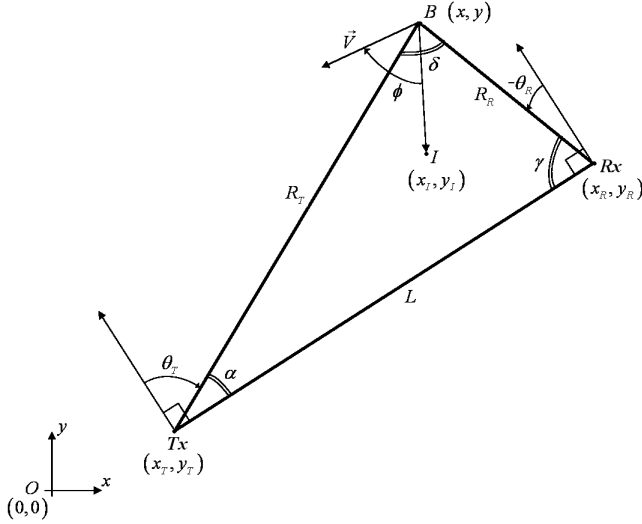


Figure 1. Bistatic geometry

From Figure 1, we have that: $\theta_T = \pi/2 - \alpha$, $\theta_R = \gamma - \pi/2$, $\delta = \pi - \alpha - \gamma = \theta_T - \theta_R$, and from the cosine law we obtain: $R_T^2 = R_R^2 + L^2 - 2R_R L \sin \theta_R$, which gives the range from transmitter to target R_T , as a function of the range from receiver to target R_R and the look angle of the receiver θ_R . In Figure 1 we plot also the target velocity vector \vec{V} ; ϕ is the angle between the target velocity vector and the bistatic bisector, which is measured in a positive clockwise direction from the bisector. In particular the bistatic bisector is represented by the vector \vec{BI} , where I is the incenter of the bistatic triangle, whose coordinates are (x, y) .

In the bistatic geometries, an important parameter is the radial velocity V_a , which is the target velocity component along the bistatic bisector. From the observation of Figure 1, we obtain $V_a = \vec{V} \cdot \vec{BI} / |\vec{BI}| = |\vec{V}| \cos \phi$.

III. BISTATIC AMBIGUITY FUNCTION

In our study we suppose that the complex envelope of the signal transmitted by the FM commercial radio station is the unitary power pulse given by:

$$u(t) = \begin{cases} \frac{1}{\sqrt{T}} e^{j\beta \sin(2\pi f_0 t + \varphi)} & |t| \leq \frac{T}{2} \\ 0 & \text{elsewhere} \end{cases} \quad (1)$$

that is a signal which instantaneous frequency is a sinusoidal oscillation [2-3]. In particular, T is the observation time, β is the modulation index and $1/f_0$ is the period of the instantaneous frequency. In other words, we assumed that, during the observation time, the modulating signal transmitted by a radio station can be approximated by a sinusoidal oscillation. This can be justified considering that in a typical FM radio, the program content is speech and/or music, which are often modelled as periodic vibrations. Moreover, the chosen signal is a mathematically tractable

model that makes it feasible to study the analyzed scenario rigorously.

As widely known, the complex ambiguity function (CAF) of a pulse $u(t)$ represents the response of a filter matched to a given finite energy signal when the signal is received with a delay τ_a and a Doppler shift ν_a relative to the nominal values τ_H and ν_H expected by the receiver. Therefore, the CAF definition is [4-5]:

$$X(\tau_H, \tau_a, \nu_H, \nu_a) = \int_{-\infty}^{+\infty} u(t - \tau_a) u^*(t - \tau_H) e^{-j2\pi(\nu_H - \nu_a)t} dt \quad (2)$$

In eq. (2), τ_a and ν_a are the actual delay and Doppler frequency of the radar target, respectively, and τ_H and ν_H are the hypothesized delay and frequency. In the monostatic case there is a linear relation between τ_a and ν_a and the target range position R_a and radial velocity V_a , i.e. $\tau_a = 2R_a/c$ and $\nu_a = 2V_a f_c/c$, where f_c is the carrier frequency of the reference signal $u(t)$. Similar relations hold for τ_H and ν_H . Clearly, $|X(\tau_H, \tau_a, \nu_H, \nu_a)|$ is maximum for $\tau_H = \tau_a$ and $\nu_H = \nu_a$.

Based upon definition (2) we can calculate the monostatic CAF for the signal $u(t)$ in eq. (1). In particular, after some manipulation, it is possible to write

$$X(\tau, \nu) = \sum_n \sum_k e^{j(n-k)\varphi} J_n(\beta) J_k(\beta) e^{+j2\pi k f_0 \tau} X_1(\tau, \nu - (n-k)f_0) \quad (3)$$

where

$$X_1(\tau, \nu) = e^{-j\pi\nu\tau} \frac{\sin(\pi\nu(T - |\tau|))}{\pi\nu T} \quad (4)$$

for $|\tau| \leq T$ and 0 elsewhere, where we set $\tau = \tau_H - \tau_a$, $\nu = \nu_H - \nu_a$ and $J_n(\beta)$ is the n^{th} order Bessel function of the first kind.

As an example, Figures 2-4 show the Ambiguity Function (AF), that is the absolute value of the CAF, of the signal in eq. (1) when $f_0 = 15\text{kHz}$, $\beta = 5$, $T = 2/f_0$ and $\varphi = \pi/2$. In particular, the 0-Doppler cut is characterized by the presence of two secondary lobes. Considering $T = k/f_0$ and $k \in \mathbb{N}$, the number of secondary lobes is $2(k-1)$.

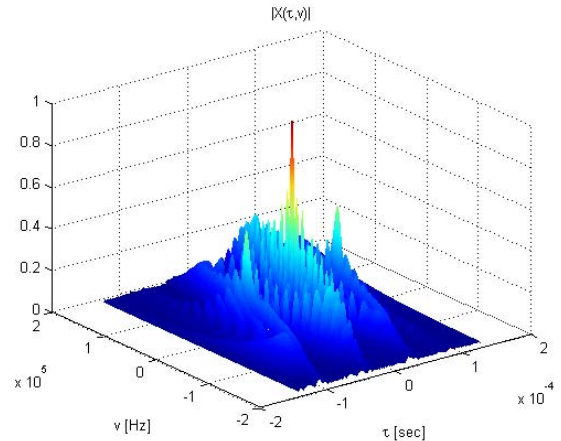


Figure 2. AF of $u(t)$, 3D-plot; $f_0 = 15\text{kHz}$, $\beta = 5$, $T = 2/f_0$, $\varphi = \pi/2$.

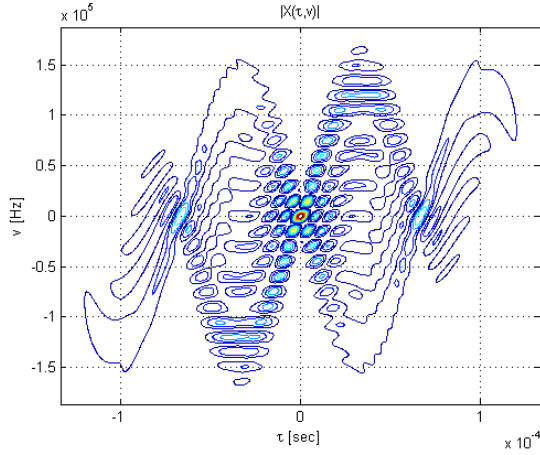


Figure 3. AF of $u(t)$, contour plot; $f_0=15\text{kHz}$, $\beta=5$, $T=2/f_0$, $\varphi=\pi/2$.

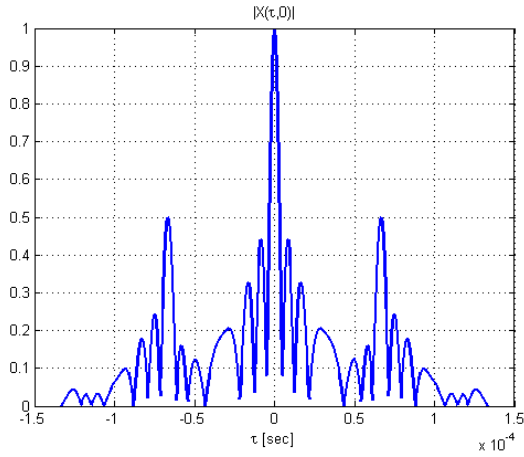


Figure 4. AF of $u(t)$, 0-Doppler cut; $f_0=15\text{kHz}$, $\beta=5$, $T=2/f_0$, $\varphi=\pi/2$.

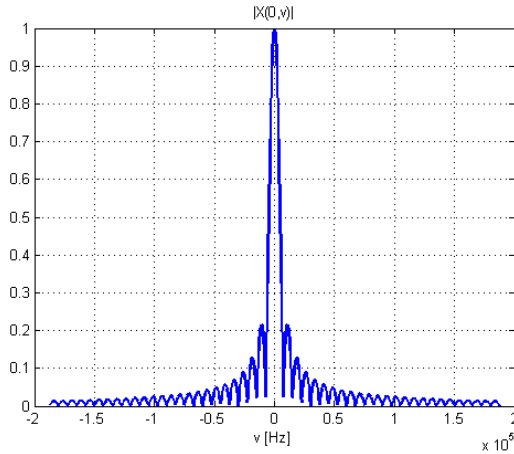


Figure 5. AF of $u(t)$, 0-delay cut; $f_0=15\text{kHz}$, $\beta=5$, $T=2/f_0$, $\varphi=\pi/2$.

The presence of secondary lobes is due to the periodicity of the analyzed pulse. Moreover, for $k>1$, the AF has a T -periodic behavior along the delay axis. Obviously, if $Tf_0 \ll 1$, $u(t)$ tends to a rectangular pulse and its CAF tends to $X_1(\tau, \nu)$ in eq. (4).

To refer eq. (3)-(4) to the bistatic geometry of Fig.1 and to obtain the expression of the bistatic ambiguity function, we must replace τ_H and ν_H in (3)-(4) with the following formulas [6],[7]:

$$\tau_H = \frac{R_R + \sqrt{R_R^2 + L^2 + 2R_R L \sin \theta_R}}{c} \quad (5)$$

and

$$\nu_H = 2 \frac{f_c}{c} V \cos \phi \sqrt{\frac{1}{2} + \frac{R_R + L \sin \theta_R}{2\sqrt{R_R^2 + L^2 + 2R_R L \sin \theta_R}}}. \quad (6)$$

Unlike the ambiguity function, which provides information on the global resolution, the CRLBs are a local measure of estimation accuracy. Anyway, both can be used to assess the error properties of the estimates of the signal parameters. In [8] the author derived a relationship between CRLB and AF, which has been successfully used in the analysis of passive and active arrays [5]. In the monostatic configuration, [8] claims that for the Fisher Information Matrix (FIM) the following relationship holds:

$$\mathbf{J}_M(\tau_a, \nu_a) = -2SNR \left[\begin{array}{cc} \frac{\partial^2 |X(\tau, \nu)|}{\partial \tau^2} & \frac{\partial^2 |X(\tau, \nu)|}{\partial \tau \partial \nu} \\ \frac{\partial^2 |X(\tau, \nu)|}{\partial \nu \partial \tau} & \frac{\partial^2 |X(\tau, \nu)|}{\partial \nu^2} \end{array} \right]_{\tau=0, \nu=0} \quad (7)$$

where SNR is the signal-to-noise power ratio at the receiver. Using the results obtained in [8], it is also possible to demonstrate that

$$-\frac{\partial^2 |X(\tau, \nu)|}{\partial \tau^2} \Big|_{\tau=0, \nu=0} = \int_{-\infty}^{+\infty} \left| \frac{\partial u(t)}{\partial t} \right|^2 dt \quad (8)$$

$$-\frac{\partial^2 |X(\tau, \nu)|}{\partial \nu^2} \Big|_{\tau=0, \nu=0} = \int_{-\infty}^{+\infty} 4\pi^2 t^2 |u(t)|^2 dt \quad (9)$$

$$-\frac{\partial^2 |X(\tau, \nu)|}{\partial \tau \partial \nu} \Big|_{\tau=0, \nu=0} = -\Im m \left\{ 2\pi \int_{-\infty}^{+\infty} t \frac{\partial u(t)}{\partial t} u^*(t) dt \right\} \quad (10)$$

After some algebra, it is possible to verify that:

$$[\mathbf{J}_M]_{1,1} = 2SNR \frac{\beta^2 2\pi f_0}{T} [2\pi f_0 T + \sin(2\pi f_0 T) \cos(2\varphi)] \quad (11)$$

$$[\mathbf{J}_M]_{2,2} = 2SNR \frac{\pi^2 T^2}{3} \quad (12)$$

$$[\mathbf{J}_M]_{1,2} = -2SNR \frac{2\beta \sin(\varphi)}{Tf_0} [\pi f_0 T \cos(\pi f_0 T) - \sin(\pi f_0 T)] \quad (13)$$

From eq. (7) the CRLBs follow:

$$\text{CRLB}(\tau_a) = [\mathbf{J}_M^{-1}(\tau_a, \nu_a)]_{1,1} \quad \text{and} \quad \text{CRLB}(\nu_a) = [\mathbf{J}_M^{-1}(\tau_a, \nu_a)]_{2,2}.$$

As an example, assuming $T=k/f_0$ ($k \in \mathbb{N}$) and considering that $\pi^2 k^2/3 \gg \sin^2(\varphi)$, the Root-CRLBs are approximated by

$$\text{RCRLB}(\tau_a) = \sqrt{\text{CRLB}(\tau_a)} \approx \frac{1}{\sqrt{2\text{SNR}}} \frac{1}{\pi B_c} \quad (14)$$

$$\text{RCRLB}(v_a) = \sqrt{\text{CRLB}(v_a)} \approx \frac{1}{\sqrt{2\text{SNR}}} \frac{\sqrt{3}}{T} \quad (15)$$

where $B_c \approx 2\beta f_0$ is Carson's Bandwidth¹ of $u(t)$. It is interesting to observe that $\text{RCRLB}(v_a)$ is inversely proportional to the time duration of the reference signal, while $\text{RCRLB}(\tau_a)$ is inversely proportional to its bandwidth. From this result we can observe that the best performance is obtained with modulating signals with high spectral content, such as rock music, and poorest performance is obtained with slow varying modulating signals, such as speech signals.

In the bistatic configuration we should express the ambiguity function in terms of the bistatic $\tau(R_R, \theta_R, L)$ and $v(R_R, V_B, \theta_R, L)$, and derive the AF with respect to the useful parameters R_R and V_B , as follows:

$$\mathbf{J}_B(R_R, V_B) = -2\text{SNR} \begin{bmatrix} \frac{\partial^2 |X(R_R, V_B)|}{\partial R_R^2} & \frac{\partial^2 |X(R_R, V_B)|}{\partial R_R \partial V_B} \\ \frac{\partial^2 |X(R_R, V_B)|}{\partial V_B \partial R_R} & \frac{\partial^2 |X(R_R, V_B)|}{\partial V_B^2} \end{bmatrix}_{R_R=R_a, V_B=V_a} \quad (16)$$

Using the derivative chain rule and letting $R_R=R_a$ and $V_B=V_a$, after some algebra it is possible to verify that [5]:

$$[\mathbf{J}_B]_{1,1} = [\mathbf{J}_M]_{1,1} \left(\frac{\partial \tau}{\partial R_R} \right)^2 + 2[\mathbf{J}_M]_{1,2} \frac{\partial \tau}{\partial R_R} \frac{\partial v}{\partial R_R} + [\mathbf{J}_M]_{2,2} \left(\frac{\partial v}{\partial R_R} \right)^2 \quad (17)$$

$$[\mathbf{J}_B]_{2,2} = [\mathbf{J}_M]_{1,1} \left(\frac{\partial \tau}{\partial V_B} \right)^2 + 2[\mathbf{J}_M]_{1,2} \frac{\partial \tau}{\partial V_B} \frac{\partial v}{\partial V_B} + [\mathbf{J}_M]_{2,2} \left(\frac{\partial v}{\partial V_B} \right)^2 \quad (18)$$

$$[\mathbf{J}_B]_{1,2} = [\mathbf{J}_M]_{1,1} \frac{\partial \tau}{\partial V_B} \frac{\partial \tau}{\partial R_R} + [\mathbf{J}_M]_{1,2} \frac{\partial \tau}{\partial R_R} \frac{\partial v}{\partial V_B} + [\mathbf{J}_M]_{1,2} \frac{\partial \tau}{\partial V_B} \frac{\partial v}{\partial R_R} + [\mathbf{J}_M]_{2,2} \frac{\partial v}{\partial R_R} \frac{\partial v}{\partial V_B} \quad (19)$$

For $L=0$ the bistatic CRLBs coincide with the monostatic CRLBs. To highlight the differences between monostatic and bistatic domain, Figures 6 and 7 show the RCRLBs as a function of the baseline length L and the angle θ_R .

It is evident that, for all the parameter values we tested, the bistatic RCRLBs are higher than the monostatic RCRLBs. The bistatic RCRLBs get even worse when the target approaches the baseline, that is when $R_R \leq L$ and θ_R approaches $-\pi/2$. In this case, the resulting delay is L/c and the radial velocity is zero, therefore resolution is totally lost and the RCRLBs tend to infinity.

¹ Carson's bandwidth rule defines the approximate bandwidth of an angle-modulated signal and is expressed by the relation $B_c = 2(\Delta f + B)$ where Δf is the peak frequency deviation, and B is the bandwidth of the modulating signal.

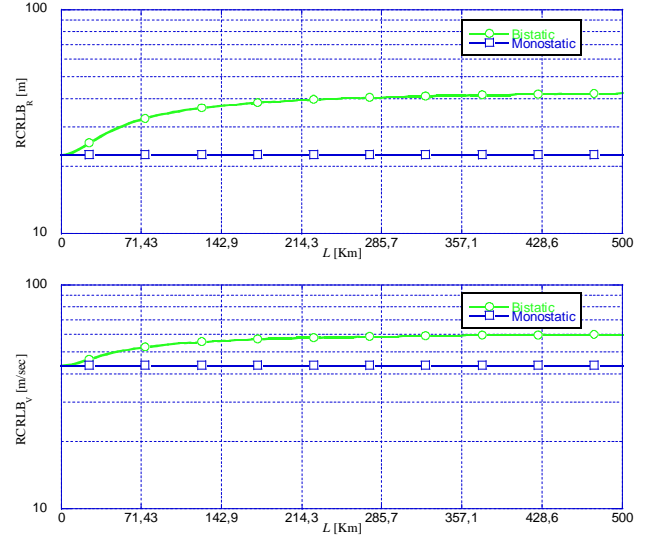


Figure 6. RCRLBs as a function of the look angle θ_R ; $L=50\text{km}$, $R_R=30\text{Km}$, $V_B=250\text{m/sec}$, $f_0=15\text{kHz}$, $\beta=5$, $T=20/f_0$, $\varphi=\pi/2$, $f_c=100\text{MHz}$, $\text{SNR}=20\text{dB}$.

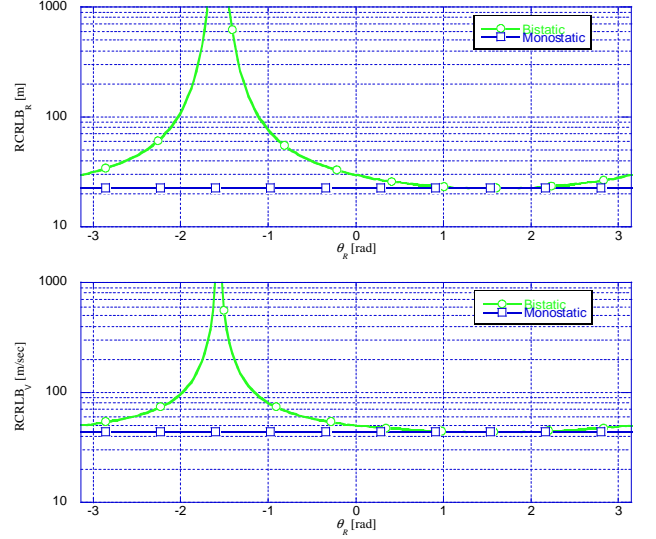


Figure 7. RCRLBs as a function of the look angle θ_R ; $L=50\text{km}$, $R_R=30\text{Km}$, $V_B=250\text{m/sec}$, $f_0=15\text{kHz}$, $\beta=5$, $T=20/f_0$, $\varphi=\pi/2$, $f_c=100\text{MHz}$, $\text{SNR}=20\text{dB}$.

IV. OPTIMAL SELECTION OF THE TX-RX PAIR

In our scenario we considered a surveillance map of dimension $L_x=100\text{km}$ and $L_y=100\text{km}$ where we placed 1 transmitter and 4 receivers.

In particular, we placed the transmitter at coordinates $T=(L_x/2, L_y/2)$ and the receivers at coordinates $R^{(1)}=(L_x/4, L_y/2)$, $R^{(2)}=(L_x/2, 3L_y/4)$, $R^{(3)}=(L_x/2, L_y/4)$ and $R^{(4)}=(3L_x/4, L_y/2)$. Therefore, there are 4 pairs of TX-RX that we considered as independent bistatic systems. The results have been obtained considering a non co-operative frequency modulated (FM) commercial radio station as transmitter of opportunity and modelling the reference signal using the pulse in eq. (1). The carrier frequency of the system was fixed to $f_c = 100\text{MHz}$, which falls within the VHF part of the radio spectrum in which FM is used for broadcasting.

In order to fix the values of f_0 and β , we considered that the signal emitted by a FM commercial radio station is an audio signal (speech and/or music), therefore the frequency of the modulating signal f_0 has to belong to the range of audio frequencies, whose accepted standard range is from 20Hz to 20kHz. Moreover, FM commercial radio stations use bandwidth of about 150kHz, therefore, according to Carson's rule, we fixed $f_0=15\text{kHz}$ and $\beta=5$.

In the analyzed scenario we also considered an omnidirectional antenna for the transmitter and directive antennas for the receivers. In particular, we considered that the antennas of the receivers have the same power gain:

$$G(\theta_R) = \begin{cases} \frac{2\pi}{2\pi - \varepsilon} \frac{2|\theta_R + \pi/2|}{\varepsilon} & |\theta_R + \pi/2| \leq \frac{\varepsilon}{2} \\ \frac{2\pi}{2\pi - \varepsilon} & \text{elsewhere} \end{cases} \quad (20)$$

that is, the receiver antenna power gain is constant for all the directions, has a notch towards the transmitter ($\theta_R = -\pi/2$) and linearly decreases when the receiver look angle belongs to the range $[-\pi/2 - \varepsilon/2; -\pi/2 + \varepsilon/2]$. In our simulation we fixed $\varepsilon = \pi/6$. We choose this receiver antenna power gain because in a real case scenario the receiver antennas are designed in order to maximize the power ratio between the target echo and the Line of Sight co-channel interference.

For each point of the analyzed area and for each of the 4 bistatic channels we calculated RCRLBs on the target range and velocity estimation accuracy. In particular, we assumed that, in each point of the analyzed area, the target has a velocity vector aligned to the x axis with intensity 250 m/sec. The RCRLBs of target range and velocity are a function of the range from the receiver to the target R_R , the baseline L , the look angle of the receiver θ_R , the radial velocity V_a , and the Signal-to-Noise Power Ratio (SNR). All these parameters depend on the configuration of the bistatic triangle, that is, on the coordinates of target, TX and RX. Bistatic geometry also affects the received echo power, because the path loss factor is $(R_T R_R)^2$. In particular, the SNR can be written as $SNR = G(\theta_R) SNR_C (L_x^2 + L_y^2)^2 / (R_T R_R)^2$, where SNR_C is a constant parameter. We assumed that $SNR_C = 20\text{dB}$. That is, we assumed that if both the transmitter and the receiver are located in $(0,0)$ and the target is located in (L_x, L_y) , then $SNR = G(\theta_R)|_{\text{dB}} + 20\text{dB}$.

Figures 8 and 11 are colour coded maps which represent the RCRLBs of the target range and the target velocity in each point of the analyzed area for the 4th bistatic system. In particular, Figure 8 represents the RCRLB of the target range, in dBm while Figure 11 represents the RCRLB of the target velocity in dBm/sec.

As apparent from the results, the RCRLBs of the bistatic system are strongly related to the bistatic geometry. It is evident that the effects of geometry factors are more prominent as the target is in the same direction of the transmitter, in this case the resolution is totally lost. This is clearly due to the geometrical factors discusses in the previous section and to the choice of the receiver antenna power gain in eq. (20). However, the effects of the bistatic

geometry are less prominent when the distance to the target increases; in this case the bistatic system behaves more and more as a monostatic system.

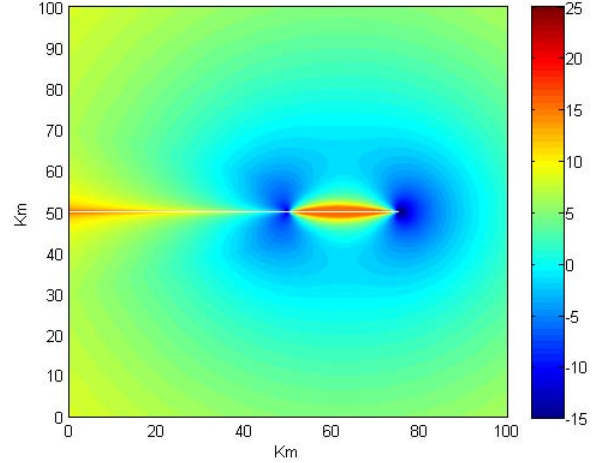


Figure 8. RCRLB of the target Range [dBm], 4th pair.

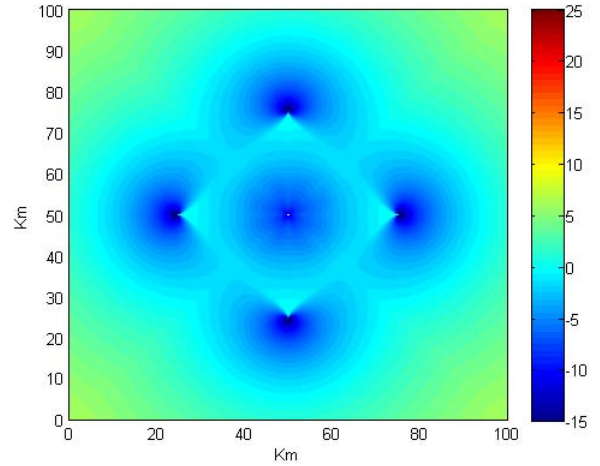


Figure 9. Minimum RCRLB of the target range [dBm].

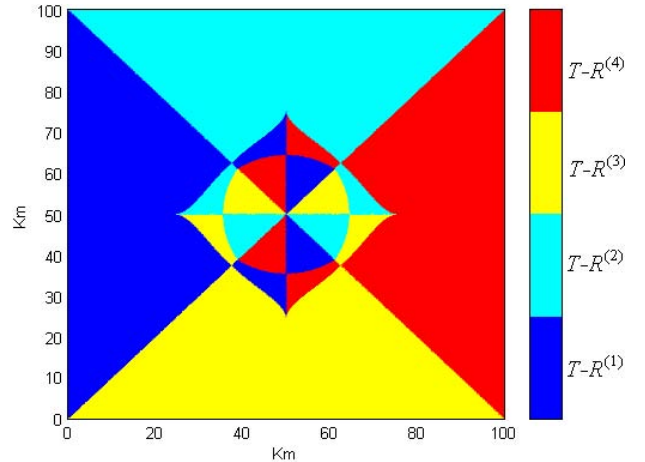


Figure 10. Optimum pair map for target range estimation.

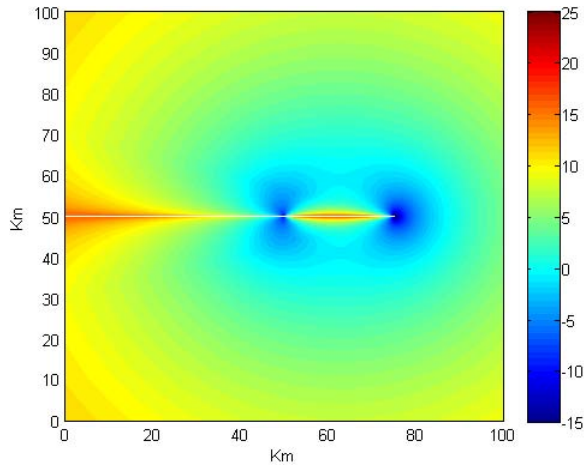


Figure 11. RCRLB of the target velocity [dBm/sec], 4th pair.

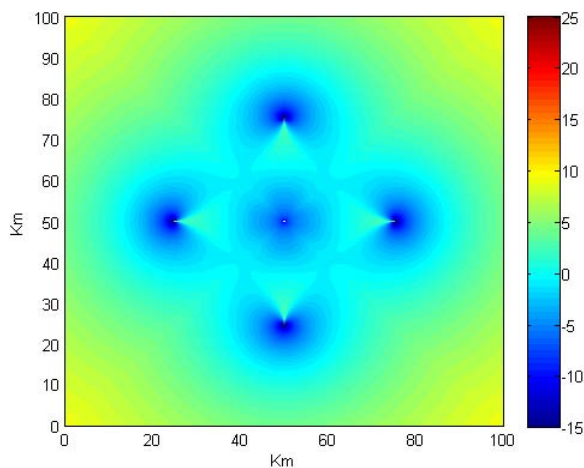


Figure 12. Minimum RCRLB of the target velocity [dBm/sec].

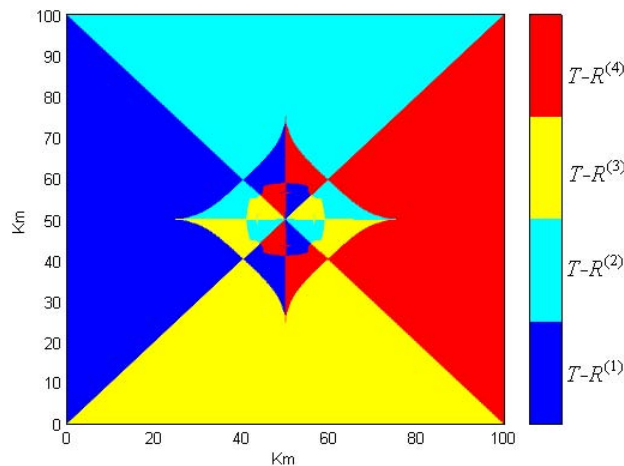


Figure 13. Optimum pair map for target velocity estimation.

Therefore, the performances of each bistatic system are strongly related to the configuration of the bistatic triangle, that is, to the positions of the transmitter, the receiver and the target. Using different transmitting and receiving systems, the target can be seen by different bistatic configurations.

Then, knowing the coordinates of each transmitter and each receiver of the whole system, it is possible to find, for each point of the analyzed area, the TX-RX pair having the best performance, in terms of the lowest RCRLB.

Figures 10 and 13 show, in a colour coded map, the transmitter-receiver pair which has the minimum RCRLB for each point of the analyzed area. The color-map of these figures is divided into 4 colours, each of which is associated with one of the 4 analyzed bistatic systems. Figures 9 and 11 show the minimum RCRLB of the target range and the target velocity, respectively, that is the value of the RCRLB which is provided by the transmitter-receiver pair which has the minimum RCRLB.

V. CONCLUSIONS

In this paper, we exploited the relation between the AF and the CRLB to calculate the bistatic CRLBs of target range and velocity. The bistatic CRLBs provide a local measure of the estimation accuracy of these parameters. Then, we used the information gained through the calculation of the bistatic CRLBs for the choice of the optimum transmit-receive pair in a multistatic radar system. The performance of each bistatic channel heavily depends upon the geometry of the scenario and the position of the target with respect to each receiver and transmitter. We approach the problem of optimally selecting the TX-RX pair based upon the CRLB for the bistatic geometry of each pair. The optimal pair was defined as that exhibiting the lowest bistatic CRLB for the target velocity or range. These results can be used for the dynamical selection of the TX-RX signals for the tracking of a radar target moving along a trajectory in a multistatic scenario. Ongoing research focuses on dynamic reconfiguration of selected TX-RX as a function of RCRLBs as well as tracking accuracy. The results reported here have been obtained considering a scenario composed of Passive Coherent Radars which exploit a single non FM commercial radio station as transmitter of opportunity.

REFERENCES

- [1] Griffiths, H.D.; Baker, C.J.; "Measurement and analysis of ambiguity functions of passive radar transmissions", Radar Conference, 2005 IEEE International, 9-12 May 2005 Page(s):321 – 325
- [2] Fulvio Gini and Georgios B. Giannakis, "Hybrid FM-Polynomial Phase Signal Modeling: Parameter Estimation and Cramér-Rao Bounds" IEEE Trans. on Signal Processing, Vol. 47, No. 2, February 1999.
- [3] G. T. Zhou, G. B. Giannakis, and A. Swami, "On polynomial phase signals with time-varying amplitudes," IEEE Trans. Signal Processing, vol. 44, pp. 848–861, Apr. 1996.
- [4] N. Levanon, E. Mozeson, Radar Signals, New York: Wiley, 2004.
- [5] A. Dogandzic, A. Nehorai, "Cramér-Rao Bounds for estimating Range, Velocity, and Direction with and Active Array", IEEE Trans. on SP, Vol. 49, No. 6, June 2001, pp. 1122-1137.
- [6] T. Tsao, M. Slamani, P. Varshney, D. Weiner, H. Schwarzlander, "Ambiguity Function for a Bistatic Radar", IEEE Trans. on AES, Vol. 33, No. 3, July 1997, pp. 1041-1051.
- [7] A. Farina, F. Gini, M. Greco, P. Stinco and L. Verrazzani, "Optimal Selection of the TX-RX Pair in a Multistatic Radar System", COGIS'09, Paris, France, November 2009.
- [8] H. L. Van Trees, Detection, Estimation and Modulation Theory. New York: Wiley, 1971, Vol. III.